ECO-DESIGN OF A SMALL SIZE INDUSTRIAL FAN FOR CERAMIC TILE COOLING

Nicola ALDI[1], Giacomo DAVOLI[2,3], Michele PINELLI[1],
Luca ROSSI[3], Alessio SUMAN[1]

[1] *Engineering Department (EnDiF), University of Ferrara, Ferrara, Italy*

[2] *Department of Engineering Enzo Ferrari, University of Modena and Reggio Emilia, Modena, Italy*

[3] *F.M. S.r.l., Correggio (RE), Italy*

SUMMARY

In this paper, the one-dimensional design and the three-dimensional numerical analysis through CFD simulations of a small size fan are carried out. The fan in consideration provides the airflow used for controlling the surface thermal gradient of ceramic tiles between the dryer and the digital printing stage. An experimental campaign performed on a backward-curved centrifugal fan prototype with an optimized air blowing device demonstrates that fan performances (efficiency and air flow rate) meet the eco-design demands and the air velocity field at the blowing device outlet is suitable to obtain the expected heat exchange. The new cooling system can also reduce acoustic emissions up to 3 dB(A) with respect to the existing one.

INTRODUCTION

The production process of ceramic tiles has remained unchanged for several decades in its main phases. Ceramic tiles are produced starting from a specific mixture of raw materials, which is pressed to obtain a green tile with poor mechanical properties. To achieve effective pressing, it is essential to maintain a certain percentage of moisture within the mixture. Then, green tiles need to be dried to facilitate the subsequent phases of decoration and firing. The decoration may provide for the application of glazes, silkscreen or digital prints and is carried out after the drying. The decoration is followed by the firing phase, which allows the obtainment of a product with the required mechanical properties and also fixes the decorations.

In recent years, ceramic tile production lines have seen the massive introduction of digital decoration. It is a technology that provides for the application of decoration on dried green tiles through an inkjet printer. To be properly decorated, the tile surface must be cooled to a temperature

between approximately 45 °C and 55 °C to achieve good ink adhesion avoiding defects such as bubbles or condensation deposits. The tile surface temperature exiting from the dryer generally ranges from about 100 °C to 120 °C. A cooling of at least 40 °C is thus needed in the line section between the dryer and the digital printer to be able to properly apply the decoration. Since in general natural convection cooling between tile surface and the surrounding air is not sufficient to ensure such a reduction of surface temperature, it is necessary to design special systems for green tile cooling.

Nowadays the cooling of dried ceramic tiles is essentially obtained through the application of two different techniques. The first technique involves the use of liquid water, which is sprayed on tiles by means of nozzles and evaporates subtracting heat from tile surface. The second technique for tile cooling uses fans, which blow air on the material to be cooled removing heat from the tile surface by forced convection.

An example of a cooling system which makes use of water is the one described by Sanchis and Peñarrocha [1], who developed and tested in a real industrial production line an automatic control system of the surface temperature of ceramic tiles by means of variable water spraying. The process consists of a transportation band that carries hot tiles through a water sprayer located after the dryer and just before the glazer. The objective of the control system is to maintain the surface temperature of tiles at the entrance to the glazer as uniform as possible to reduce the percentage of defects associated with temperature variations. The adaptive control is based on surface temperature measurements upstream and downstream the water sprayer. The regulation of the quantity of water deposed (and hence evaporated) on each tile allows the control of its surface temperature. This quantity is regulated by changing the velocity of the transportation band and the sprayer flow.

The ceramic tile cooling system analyzed in this paper, widely used in the section of the production line between the dryer and the digital printer, involves the use of centrifugal fans arranged in series and equipped with special blowing devices able to create an air knife which removes heat from the tile surface by forced convection (see Fig. 1a).

In order to define the process requirements, and therefore the required performances for the cooling system in consideration, a finite difference model of tile heat transfer, which allows the calculation of the temperature gradient across tile thickness, has been developed. By means of this model, it has been possible to conduct a numerical Design of Experiments (DOE) study, which allowed the quantification of the effect on tile cooling of the most significant variables related to the cooling system, the production line and the work environment respectively. For the full factorial DOE application, five variables have been identified: the fan volume flow rate, the mean air velocity at the blowing device outlet, the production line speed, the distance between two adjacent fans and the initial temperature difference between tile surface and ambient air. Three values for each of the considered variables have been chosen, which are representative of the actual range of working conditions.

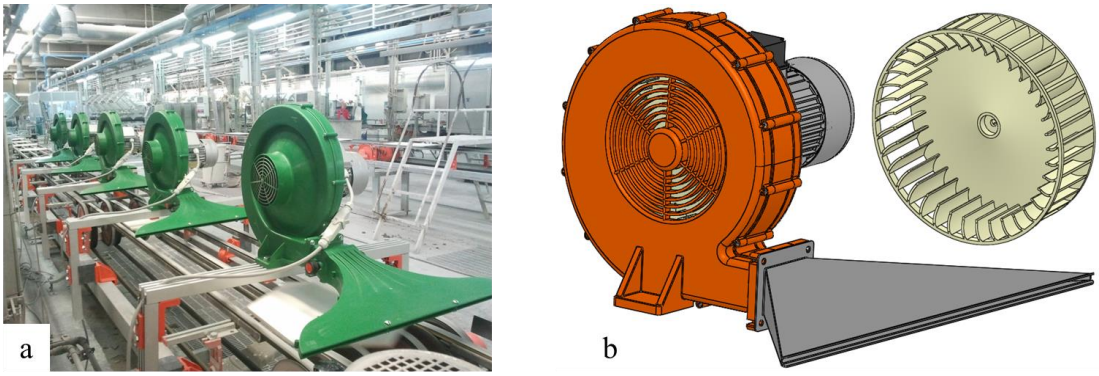

Figure 1: a) ceramic tile cooling by means of centrifugal fans arranged in series and b) existing cooling system and Sirocco impeller (courtesy of F.M. S.r.l.)

It has been observed that the mean air velocity at the blowing device outlet, $\overline{V}$, is the variable which mostly influences the tile surface temperature. This result is due to the fact that convective heat transfer, and therefore tile cooling, is strongly affected by the speed with which the fluid approaches the surface. Moreover, the simulations performed by means of the numerical model for tile heat transfer allowed the establishment of the minimum value of $\overline{V}$ necessary to obtain the tile cooling required by the process. This pre-established threshold minimum value, $\overline{V}_{\text{th}}$, represents a performance target for the cooling system under study.

In this paper, the fluid dynamic design of a small size centrifugal fan is presented. The considered fan provides the airflow used for controlling the surface thermal gradient of ceramic tiles between the dryer and the digital printing stage. At first, an experimental characterization of the existing Sirocco type fan and the coupled blowing device is carried out, to assess the ability of the existing system to obtain the tile cooling required by the process. A new backward-curved type fan is then designed, in the light of a recent European Directive on eco-design demands for fans. The new design is performed by means of an integrated one-/three-dimensional procedure. In particular, the performance specifications for the one-dimensional design are defined starting from the results of the numerical study previously described, while the three-dimensional numerical analysis is based on the use of CFD simulations. Finally, an experimental campaign on a backward-curved fan prototype with an optimized air blowing device is carried out, to evaluate whether fan performances (efficiency and air flow rate) meet the eco-design demands and the air velocity field at the blowing device outlet is suitable to obtain the expected heat exchange.

EXISTING COOLING SYSTEM CHARACTERIZATION

The existing ceramic tile cooling system is shown in Fig. 1b. It consists of a Sirocco type fan equipped with a special blowing device able to create an air knife which removes heat from the tile surface by forced convection.

The Sirocco fan, also known as squirrel-cage fan, is a forward-curved centrifugal fan. Fans of this type are used in a variety of applications requiring compactness, low noise, relatively high flow rate and low cost (e.g. heating, ventilating, conditioning and cooling). In literature, peak efficiencies ranging from 50 % (typical) to 70 % (maximum) are reported [2], which are somewhat lower than that of other types of centrifugal fans in the same size class.

As reported by Eck [3], the main features of the Sirocco impeller are its large inlet-to-outlet diameter ratio, D_1/D_2, and its large number of short-chord blades. The great number of blades is used to counterbalance the deficient flow guiding resulting from their short radial length and strong curvature. Nevertheless, since the airflow within blade channels can hardly follow the strong curvature of the blades, the flow is far from smooth and this is the main reason for the lower efficiency of Sirocco fans. Stepanoff [4] also pointed out that one of the drawbacks of this type of fans is their narrow range of operation and that on both sides of the best efficiency point the fan becomes noisy.

Several experimental investigations have been conducted on Sirocco type fans to better understand the main characteristics of their complex internal flow. Cabitza et al. [2] and Kind and Tobin [5] observed a strong flow separation at the shroud region, with substantial axial and circumferential non-uniformity of both the inlet and outlet flow-field, and reverse flow over much of the operating range. The coexistence of a strongly curved meridional flow and separated regions cause the generation of three-dimensional effects [2].

The Sirocco fan under examination is composed of a constant-width unshrouded impeller (see Fig. 1b), with a diameter ratio D_1/D_2 equal to 0.82, and a constant-width spiral volute, both produced through thermoplastic injection molding. The blade mean line is a single circular arc. The fan is

driven directly by a two-pole three-phase asynchronous electric motor with a rated power of 1.1 kW.

Fan experimental characterization

In order to characterize the performances of the existing Sirocco fan, an experimental campaign is carried out. A test rig, schematically illustrated in Fig. 2, is built for this purpose in accordance with the European Standard EN ISO 5801.

The test rig is composed of a straight duct connected to the fan through a divergent transition section. Since the fan inlet is open to the atmosphere, the static pressure rise produced by the fan is determined by measuring the relative static pressure $(p_g)_{out}$. The fan volume flow rate Q is measured with a calibrated orifice plate having a diameter ratio equal to 0.75, designed according to the European Standard EN ISO 5167-2. The D and $D/2$ tap configuration is used for the orifice plate static pressure drop Δp_{or} measurement. In order to define the thermodynamic state of the air upstream the orifice plate, the static temperature $(T)_{up}$ and the static pressure $(p_g)_{up}$ need to be measured. A type K thermocouple is used for this purpose, while all pressure measurements are performed by means of differential pressure transducers. A throttling valve is installed at the exit of the duct, allowing the fan operating point to be varied. Since the throttling of the valve causes little variations of the rotational speed of the electric motor shaft, the rotational speed is measured for each operating point with a stroboscope. A three-phase energy analyzer is used to measure the electric power P_e supplied to the motor. Ambient conditions, i.e. pressure, temperature and relative humidity, are recorded during experimental tests by means of a barometric station.

Experimentally measured fan performances are expressed in terms of flow coefficient ϕ and pressure coefficient ψ, which are defined according to Eck [3] as:

$$\phi = \frac{4Q}{\pi U_2 D_2^2} \tag{1}$$

$$\psi = \frac{2\Delta p_0}{\rho U_2^2} \tag{2}$$

where U_2 is the blade velocity at impeller outlet, Δp_0 is the fan total pressure rise and ρ is the air density.

The results of the experimental campaign are reported in Fig. 3a, in which the best efficiency point (BEP) is also marked. In particular, the ratio η_{BEP}/η_{target} is indicated, where η_{BEP} is the overall efficiency η at the BEP calculated as:

$$\eta = \frac{\Delta p_0 Q}{P_e} \tag{3}$$

and η_{target} is the target energy efficiency calculated in accordance with the European Regulation 327/2011 [6] on eco-design requirements for fans driven by electric motors with an input power

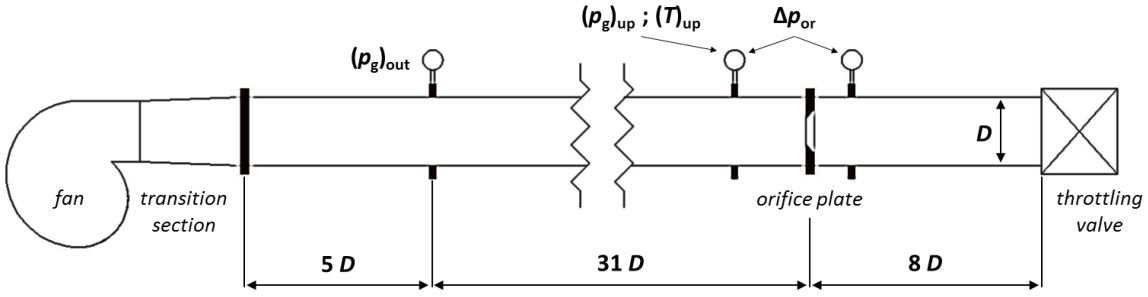

Figure 2: test rig and sensor positions

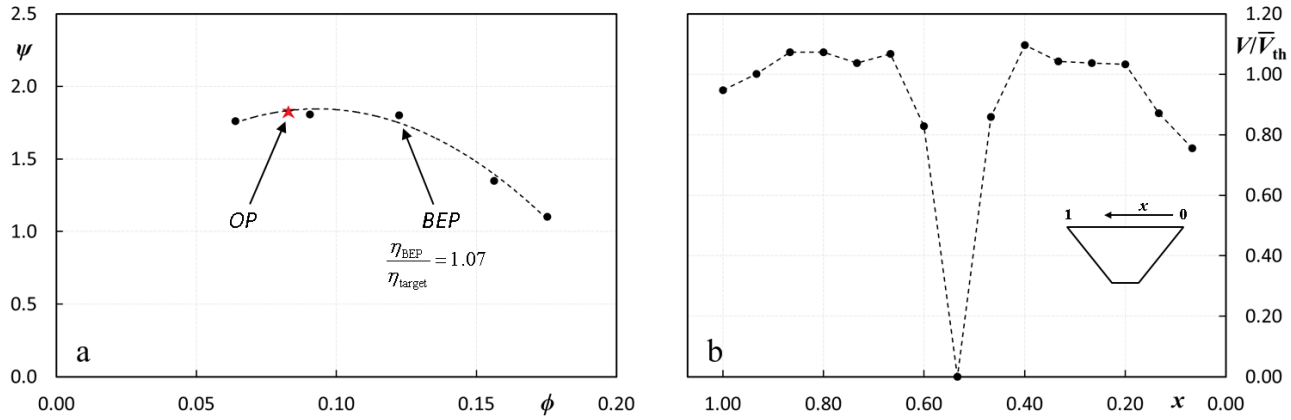

Figure 3: existing cooling system experimental performances: a) fan characteristic curve and b) non-dimensional velocity distribution at the blowing device outlet section

between 125 W and 500 kW. The target energy efficiency η_{target} depends on the fan type and the electric power supplied to the motor.

Since $\eta_{BEP}/\eta_{target} > 1$, the performances of the existing Sirocco fan comply with the eco-design demands set out in the aforementioned European Regulation.

Blowing device experimental characterization

As highlighted above, since for the ceramic tile cooling system under study the tile cooling is obtained by forced convection, the air velocity at the blowing device outlet has a great influence on the tile surface temperature.

In order to assess the suitability of the outlet air velocity field to obtain the expected heat exchange, an experimental characterization is carried out on the existing blowing device coupled to the Sirocco fan. The local air velocities are measured along the centerline of the blowing device outlet section by means of a Pitot tube and are expressed in terms of the non-dimensional ratio $V/\overline{V}_{th}$ between the local air velocity V and the threshold minimum value $\overline{V}_{th}$ previously established. The results of the experimental tests are reported in Fig. 3b.

It can be observed that the local air velocity V is lower than the threshold value $\overline{V}_{th}$ at the ends and in the center of the blowing device outlet section. In particular, the lower air velocities in the center of the outlet section are due to the presence of a local stiffening strut, orthogonally disposed with respect to the flow direction, whose function is to limit the deformation of the blowing device during operation. Since this local stiffening strut is a blunt-shaped body, it results in a wide wake region. Furthermore, the flow is highly non-uniform on the considered section.

The operating point (OP) of the Sirocco fan coupled to the existing blowing device is also marked in Fig. 3a. It is possible to notice that the flow coefficient ϕ at the OP is lower compared to that at the BEP.

Therefore, even though the performances of the Sirocco fan meet the European eco-design demands for fans, the air velocity distribution at the coupled blowing device outlet does not appear to be suitable for obtaining the tile cooling required by the process, especially in the light of increasingly higher production line speeds. Moreover, the matching between the fan OP and its BEP is not optimal.

A new cooling system is thus designed to fulfil the process requirements. The possibility of reducing the rated power of the electric motor that drives the fan is also evaluated. Since electric motor efficiencies decrease with their size, a different fan type needs to be considered to design a machine that complies with the European Regulation on eco-design demands for fans. A backward-

curved type centrifugal fan is designed for this purpose. This type of fan, in fact, is characterized by peak efficiencies higher than that of forward-curved fans [4, 7]. The new cooling system should also reduce acoustic emissions with respect to the existing one.

NEW COOLING SYSTEM DESIGN

The fluid dynamic design of the new cooling system is performed by means of an integrated one-/three-dimensional procedure. In particular, the three-dimensional numerical analysis is based on the use of CFD simulations.

Centrifugal fans have historically been aerodynamically designed according to the assumption of one- or two-dimensional ideal flow, corrected with the use of empirical correlations [3]. The main components of the fan (i.e. inlet cone, impeller and volute) are individually designed and their interactions are neglected [3]. However, the real flow is far from the ideal situation and therefore it is not possible to predict the fan performances at the design stage. In fact, the nature of the flow-field within a centrifugal fan is highly three-dimensional, as the flow is turned from axial to radial direction. Moreover, the effect of interactions between stationary and rotating components on fan performances should be taken into account.

In this context, CFD numerical simulations have been established, as compared to experimental techniques, as the baseline approach to predict the three-dimensional flow-field in radial turbomachines. For instance, Zhao et al. [8] numerically computed the flow-field for a whole centrifugal fan to analyze the interactions between inlet cone, impeller and volute. Ng and Damodaran [9] investigated the performance characteristics of an industrial centrifugal fan using a sliding mesh CFD model. Recently, Corsini et al. [10] carried out the numerical investigation of the flow-field in a high-pressure centrifugal fan for the process industry, to highlight the critical regions inside the device and suggest possible modifications to increase its duty life.

CFD is thus considered a key tool which can complement traditional one- or two-dimensional design approaches. Comprehensive information on the use of CFD in centrifugal fan optimization is reported by Tallgren et al. [11]. In recent works, examples of advanced use of CFD regarding optimization of industrial centrifugal fans can be found in [12], [13] and [14]. In particular, Ferrari et al. [13] and Pinelli et al. [14] presented the fluid dynamic design of centrifugal fans by means of an integrated one-/three-dimensional numerical procedure based on the use of CFD simulations.

Fan one-dimensional design

The performance specifications for the one-dimensional design of the new backward-curved centrifugal fan are defined starting from the results of the simulations performed by means of the numerical model for tile heat transfer previously described. The design performances, in terms of flow coefficient ϕ and pressure coefficient ψ, are $\phi_d = 0.045$ and $\psi_d = 1.15$ respectively. The rated power of the two-pole three-phase asynchronous electric motor directly coupled to the fan is reduced from 1.1 kW to 0.37 kW.

Since fan components will be produced through thermoplastic injection molding, geometrical constraints are set to the achievable shape and thickness for the components. In particular, an unshrouded impeller with simple curvature blades needs to be designed. Furthermore, to ensure the perfect interchangeability with the existing fan model, the outlet section of the volute must be maintained in its shape and dimensions.

The fan one-dimensional design is carried out by means of the procedure proposed by Eck [3]. In accordance with the one-dimensional ideal flow theory, the fluid is assumed to enter and leave an impeller passage tangential to the blade profile. The flow is also assumed to be uniform at each section and viscous losses are neglected.

The application of Eck's procedure results in an impeller geometry (see Fig. 4a) characterized by a diameter ratio D_1/D_2 and a width ratio b_2/b_1 equal to 0.45 and 0.40 respectively. The relative tip clearance a, defined as the ratio between the tip clearance δ and the average blade width $(b_1+b_2)/2$:

$$a = \frac{\delta}{(b_1 + b_2)/2} \tag{4}$$

is equal to 0.10. The blade mean line is a single circular arc.

A volute with a rectangular cross-section (see Fig. 4b) is then designed according to Eck [3]. The individual rectangular section is altered radially and axially with the θ angle so that it results in geometrically similar sections. In this way, the ratio between the height h and the width b of each section is a constant. As can be seen from Fig. 4b, the inlet cone is integrated in the volute.

Fan CFD analysis

As stated above, the real flow within a centrifugal fan is far from the ideal situation assumed at the design stage and the interactions between fan components are not negligible. In the present study, the existence of a tip clearance makes the flow in an impeller passage more complex. In this regard, comprehensive experimental and numerical studies of the effects of tip clearance on the performances of centrifugal fans with unshrouded impellers can be found in [15] and [16].

In order to assess the performances of the centrifugal fan previously designed and analyze its three-dimensional internal flow-field, a CFD numerical simulation is performed at the fan design point. The CFD simulation is carried out on a computational domain composed of two stationary domains (inlet cone and volute) and one rotating domain (impeller). To reduce the computational effort, only one blade passage is modeled for the impeller and only a section of the same angular extent is modeled for the inlet cone. Moreover, the inlet cone and volute domains are intentionally extended to properly apply the inflow and outflow boundary conditions. In Fig. 5a, a sketch of the computational domain is represented.

The numerical simulation is performed with the commercial CFD code ANSYS CFX 15.0, which solves the 3D Reynolds-averaged form of the Navier-Stokes equations by using a finite-element based finite-volume method. A second-order high-resolution advection scheme is adopted to calculate the advection terms in the discrete finite-volume equations.

A hybrid grid, generated by means of ANSYS Meshing 15.0, with a total number of 17,391,949 elements is used in the simulation. Six prism layers are added on the surface of the blade to help solve the boundary layer around the blade. An enlarged view of the mesh on the blade surface is shown in Fig. 5b. The clearance at the impeller tip is resolved with 14 nodes across the gap span. A one-to-one node matching periodicity is also used.

The turbulence model used in the calculation is the standard k-ε model and near-wall effects are

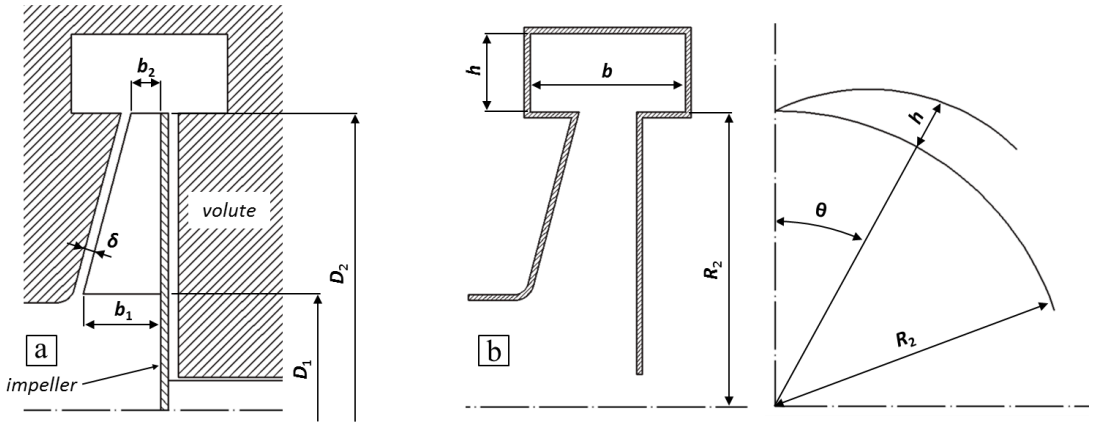

Figure 4: fan one-dimensional design: a) impeller geometry and b) volute geometry

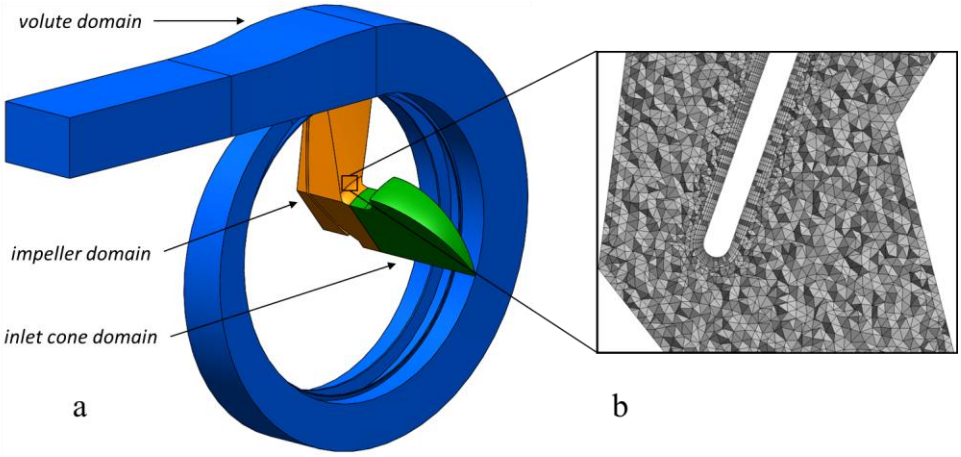

Figure 5: fan CFD analysis: a) computational domain and b) numerical grid on the blade surface

modeled with scalable wall functions. In recent years, the *k-ε* model has been more widely used in numerical simulation of turbomachines. For example, Thakur et al. [17] demonstrated the validity of the *k-ε* model in the prediction of overall performances of a centrifugal blower near the design point.

The simulation is carried out in a steady multiple frame of reference, taking into account the contemporary presence of moving and stationary domains. In particular, a mixing plane model is imposed at the interfaces between rotating and stationary domains. This rotor/stator interaction model can predict the correct trends in all global measures of performance, as proved by Thakur et al. [17] for centrifugal blowers.

Since the maximum local Mach number is lower than 0.15, the incompressible flow hypothesis is adopted. A zero relative total pressure and the flow angle are applied at the inflow boundary, while at the outflow boundary the design mass flow rate is imposed. The considered rotational speed is that of the design. Finally, since only a section of the impeller and inlet cone geometries are modeled, rotational periodic boundary conditions are applied to the lateral surfaces of the correspondent flow domains.

Regarding overall performances of the centrifugal fan at the design point, the numerically predicted pressure coefficient ψ is equal to 1.09. This value is 5.2 % lower compared to that fixed at the design stage. In order to understand the reasons for this difference in fan performances, it is necessary to analyze its three-dimensional flow-field.

The static pressure field within the fan and the relative velocity field along the blade passages, both normalized by dividing with respect to the correspondent maximum values, are reported in Fig. 6 on a two-dimensional section orthogonal to the axis of rotation and located at 50 % of the blade span.

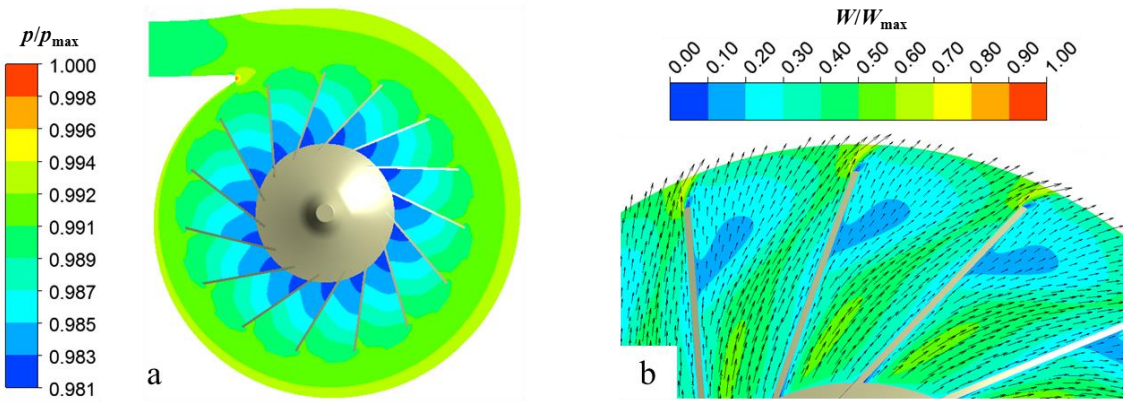

Figure 6: a) static pressure field within the fan and b) relative velocity field along the blade passages

In Fig. 6a, the static pressure rise within the impeller due to the diffusion process and the action of the centrifugal force field can be clearly observed. The static pressure progressively increases in the volute, while in the final convergent section of the volute the static pressure decreases and the fluid velocity increases. It is also possible to notice a local increase of the static pressure in correspondence of the volute tongue, caused by the stagnation of the flow. Although no flow separation from the blade profile occurs, the distribution of the relative velocity magnitude along the blade passages shown in Fig. 6b is distorted by three-dimensional effects related to the existence of a tip clearance.

In order to illustrate the evolution of the relative flow trajectories within adjacent blade vanes, the three-dimensional streamlines through the impeller are drawn in Fig.7a. As can be seen, the flow patterns are completely three-dimensional and the complexity of the flow-field is mainly caused by the leakage flow across the tip clearance, induced by the pressure difference between the two sides of the blade at the tip. The relative flow structure is clarified by Fig. 7b, in which relative velocity contours and vectors on three cylindrical sections of the impeller are represented. In particular, the considered cylindrical sections are located at 10 %, 50 % and 90 % of the blade passage radial length respectively. Moving towards higher radial positions, it can be noticed that: (i) the local leakage velocity increases, since the local pressure difference between the two surfaces of the blade increases, and (ii) the distortion of the main flow due to the interaction with the leakage flow is more evident (see Fig. 6b), since the local relative tip clearance δ/b (where b is the local blade width) increases. These phenomena are confirmed by Lakshminarayana [18], who observed that the two most critical parameters controlling the magnitude of the leakage flow are blade clearance height and the blade loading.

Furthermore, analyzing the relative velocity contour on the cylindrical section at 10 % of the passage radial length, it can be seen that the leakage flow tends to move farther along the tangential direction before interacting with the main flow. This results in very low relative velocities in the interaction region, which is located close to mid-passage. The same situation is noticed by Lakshminarayana [18] in an axial flow compressor rotor.

Blowing device optimization

In order to investigate the characteristics of the flow within the existing blowing device, CFD numerical simulations are performed considering different flow rates.

To reduce the computational effort, only a quarter of the blowing device geometry is modeled. Moreover, the presence of the local stiffening strut at the exit of the device is not considered. The numerical simulations are carried out with ANSYS CFX 15.0. A second-order high-resolution advection scheme is adopted to calculate the advection terms in the discrete finite-volume equations. A hexahedral grid, generated by means of ANSYS ICEM CFD 15.0, with a total number of 6,784,755 elements is used in the simulations. The turbulence model used in the calculations is

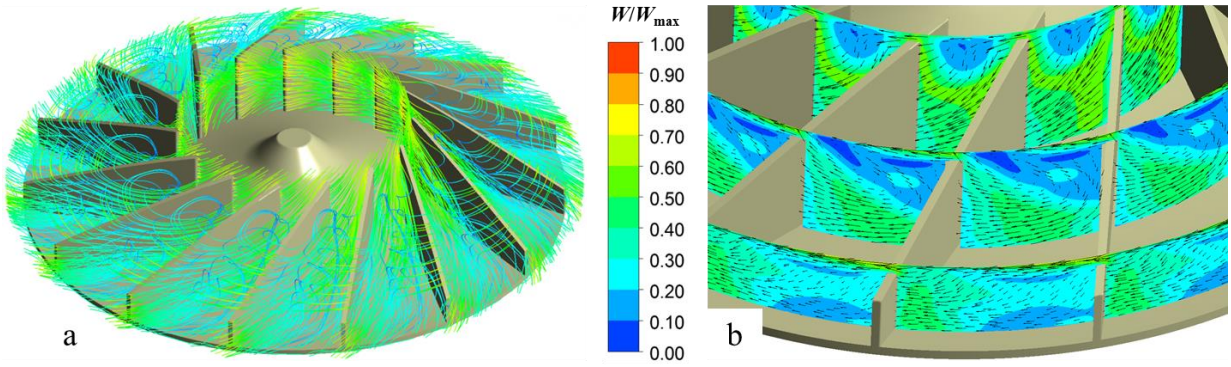

Figure 7: a) three-dimensional streamlines through the impeller and b) tomography of the leakage flows

the standard *k-ε* model and near-wall effects are modeled with scalable wall functions. The incompressible flow hypothesis is adopted. The mass flow rate and the flow angle are imposed at the inflow boundary, while at the outflow boundary a zero relative static pressure is applied. Finally, since only a section of the full geometry is modeled, symmetry boundary conditions are imposed at the correspondent surfaces.

The velocity field within the blowing device, normalized by dividing with respect to its maximum value, is reported in the left part of Fig. 8a on the horizontal plane of symmetry of the device. The velocity contour corresponds to the design volume flow rate Q_d of the designed centrifugal fan. The presence of a wide separated flow region can be observed in correspondence to the lateral surface of the blowing device. This flow separation is caused by a sudden expansion of the device section and is felt by the coupled fan as a pressure loss. It is also noticed that the extension of this separation zone does not change as the flow rate varies.

Starting from the last observation, the blowing device geometry is optimized. In particular, only the lateral surface profile is modified on the basis of the characteristics of the separation region detected through the CFD analysis. The velocity field within the optimized blowing device is shown in the right part of Fig. 8a. It can be seen that the flow is smooth and no separation from the lateral surface of the device occurs.

The comparison between the internal losses of the existing and optimized blowing devices is carried out taking into consideration the total pressure losses Δp_{0loss}, non-dimensionalized by dividing with respect to the inlet relative total pressure $(p_{0g})_{in}$. In Fig. 8b, the ratio $\Delta p_{0loss}/(p_{0g})_{in}$ is reported as a function of the non-dimensional ratio Q/Q_d. It can be observed that the optimized blowing device is characterized by lower total pressure losses with respect to the existing one in the whole range of flow rate explored.

NEW COOLING SYSTEM CHARACTERIZATION

A prototype of the designed centrifugal fan with the optimized air blowing device is tested to evaluate the performances of the new cooling system. The fan characteristic curve and the non-dimensional velocity distribution along the centerline of the blowing device outlet section are shown in Fig.9.

It can be noticed that the experimentally determined pressure coefficient ψ at the fan design point is equal to 1.04 (see Fig. 9a). This value is 9.6 % lower compared to that fixed at the design stage and 4.6 % lower compared to that numerically predicted. In the latter case, the difference is probably related to the different way with which experimental performances are determined with respect to numerical performances.

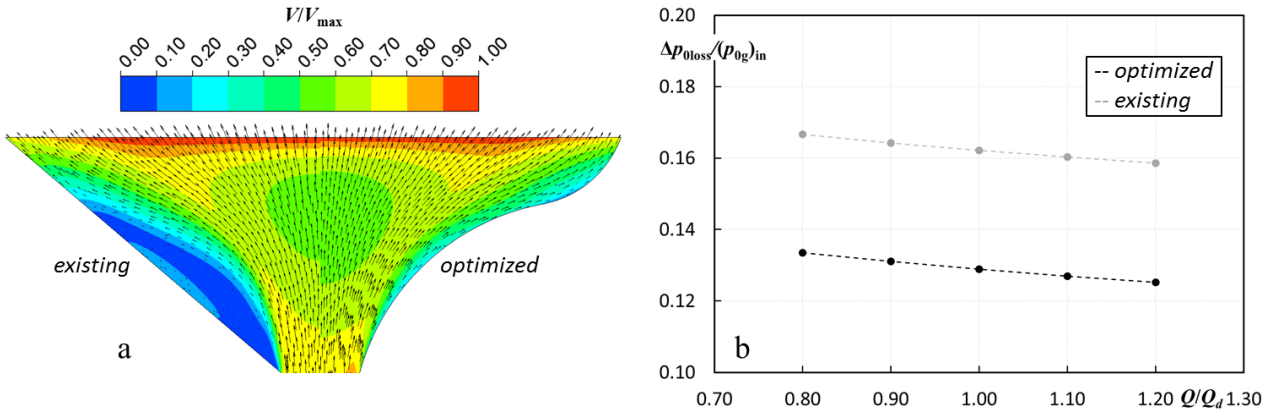

Figure 8: blowing device CFD analysis: a) velocity field and b) total pressure losses

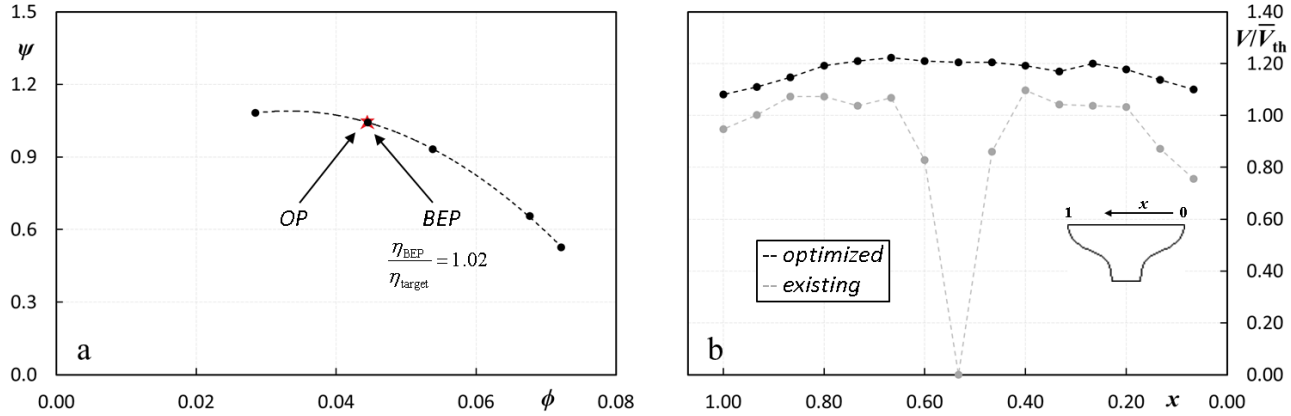

Figure 9: new cooling system experimental performances: a) fan characteristic curve and b) non-dimensional velocity distribution at the blowing device outlet section

Since $\eta_{BEP}/\eta_{target} > 1$, the performances of the designed fan comply with the eco-design demands set out in the European Regulation 327/2011. This ratio is lower than that calculated for the existing Sirocco fan. However, it is necessary to point out that: (i) the target energy efficiency η_{target} fixed by the European Regulation for a backward-curved type centrifugal fan is higher and (ii) the efficiency of the electric motor coupled to the designed fan is lower due to its smaller size. Therefore, the increase in the fan efficiency obtained is remarkable. Furthermore, the OP of the designed fan coupled to the optimized blowing device matches the fan BEP (see Fig. 9a). This aspect is particularly important for the purpose of energy saving, as the ceramic tile cooling system analyzed in this work involves the use of centrifugal fans arranged in series.

Examining the velocity distribution reported in Fig. 9b, it is possible to observe that the local air velocity V is higher than the threshold value $\overline{V}_{th}$ on the whole outlet section of the blowing device. In this case, the presence of the local stiffening strut does not result in an appreciable wake region, since its shape is aerodynamically designed. The flow is also uniform on the considered section. The air velocity distribution at the outlet section of the optimized blowing device is therefore suitable for obtaining the tile cooling required by the process.

Finally, an experimental characterization of the acoustic emissions is performed on the existing and new cooling systems in accordance with the European Standard EN ISO 3746. The new cooling system is able to reduce acoustic emissions up to 3 dB(A) with respect to the existing one.

BIBLIOGRAPHY

[1] R. Sanchis, I. Peñarrocha, *Control of a ceramic tiles cooling process based on water spraying*, Journal of Process Control, 19(7), pp. 1073-1081, **2009**

[2] S. Cabitza, F. Nurzia, C. Palomba, P. Puddu, *Detailed experimental investigation of the flow field during design and off-design operation of a squirrel cage fan*, Proceedings of the International Conference on Fans, London, UK, **2004**

[3] B. Eck, *Fans*, Pergamon Press, New York, USA, **1973**

[4] A. J. Stepanoff, *Turboblowers*, John Wiley & Sons, Inc., New York, USA, **1955**

[5] R. J. Kind, M. G. Tobin, *Flow in a Centrifugal Fan of the Squirrel-Cage Type*, Journal of Turbomachinery, 112(1), pp. 84-90, **1990**

[6] Commission Regulation (EU) No 327/2011, **2011**

[7] F. P. Bleier, *Fan Handbook*, McGraw-Hill, New York, USA, **1998**

[8] Y. Zhao, L. Song, H. Wenqi, W. Weixiong, H. Dongtao, Z. Zhichi, *Numerical Simulation of Flow Field for a Whole Centrifugal Fan and Analysis of the Effects of Blade Inlet Angle and Impeller Gap*, HVAC&R Research, 11(2), pp. 263-283, **2005**

[9] W. K. Ng, M. Damodaran, *Computational flow modeling for optimizing industrial fan performance characteristics*, European Conference on Computational Fluid Dynamics, ECCOMAS CFD 2006, Egmond aan Zee, The Netherlands, **2006**

[10] A. Corsini, G. Delibra, F. Rispoli, A. G. Sheard, P. Venturini, *Aerodynamic simulation of a high-pressure centrifugal fan for process industries*, Proceedings of ASME Turbo Expo 2013, San Antonio, Texas, USA, **2013**

[11] J. A. Tallgren, D. A. Sarin, A. G. Sheard, *Utilization of CFD in development of centrifugal fan aerodynamics*, Proceedings of the International Conference on Fans, London, UK, **2004**

[12] Y. T. Lee, V. Ahuja, A. Hosangadi, M. E. Slipper, L. P. Mulvihill, R. Birkbeck, R. M. Coleman, *Impeller Design of a Centrifugal Fan with Blade Optimization*, International Journal of Rotating Machinery, 2011, pp. 1-16, **2011**

[13] C. Ferrari, M. Pinelli, P. R. Spina, P. Bolognin, L. Borghi, *Fluid dynamic design and optimization of two stage centrifugal fan for industrial burners*, Proceedings of ASME Turbo Expo 2011, Vancouver, British Columbia, Canada, **2011**

[14] M. Pinelli, C. Ferrari, A. Suman, M. Morini, M. Rossini, *Fluid dynamic design and optimization of a double entry fan driven by tractor power take off for mist sprayer applications,*, Proceedings of the International Conference on Fans Noise, Technology and Numerical Methods, Senlis, France, pp. 1-12, **2012**

[15] T. Engin, M. Gur, R. Scholz, *Effects of tip clearance and impeller geometry on the performance of semi-open ceramic centrifugal fan impellers at elevated temperatures*, Experimental Thermal and Fluid Science, 30, pp. 565-577, **2006**

[16] T. Engin, *Study of tip clearance effects in centrifugal fans with unshrouded impellers using computational fluid dynamics*, Journal of Power and Energy, 220, pp. 599-610, **2006**

[17] S. Thakur, W. Lin, J. Wright, *Prediction of Flow in Centrifugal Blower Using Quasi-Steady Rotor-Stator Models*, Journal of Engineering Mechanics, 128(10), pp. 1039-1049, **2002]**

[18] B. Lakshminarayana, *Fluid Dynamics and Heat Transfer of Turbomachinery*, John Wiley & Sons, Inc., New York, USA, **1996**